



# Ligamental compartments and their relation to the passing spinal nerves are detectable with MRI inside the lumbar neural foramina

Dina Wiersbicki<sup>1</sup> · Anna Völker<sup>2</sup> · Christoph-Eckhard Heyde<sup>2</sup> · Hanno Steinke<sup>1</sup>

Received: 28 November 2018 / Revised: 26 May 2019 / Accepted: 28 May 2019 / Published online: 17 June 2019  
© Springer-Verlag GmbH Germany, part of Springer Nature 2019

## Abstract

**Purpose** Intraforaminal ligaments (IFL) in lumbar neural foramina (NF) and their relation to the lumbar spinal nerves (SN) are addressed.

**Method** Giemsa- and PAS-stained plastinated body slices of 15 lumbar spines were made and compared to MRI and CT data acquired of the same fresh specimens. We dissected one fixed lumbar spine to discuss our results with previous literature. Macroscopic pathophysiological changes and operational interventions at these lumbar spines were excluded.

**Results** In the NF, thin medial IFL touch the SN. As a second compartment, intermedial vertical IFL are seen. A third lateral horizontal compartment of IFL is formed by thick cranial and caudal ligaments. Ligaments of the second and third compartments have no direct contact with the SN. From medial to lateral, the IFL thicken. All compartments are 3D reconstructed. If compartments of the IFL have no direct contact with the SN seen in the slices, a connection was noticed after dissection.

**Conclusion** Manual dissection seems to be inappropriate for a detailed study of the IFL. The lateral and intermedial compartments being free of the SN may transmit power and protect the SN, while the thin medial IFL may lead the SN passing the NF under physiological conditions. We conclude from the close topographical relation that the IFL may be relevant in foraminal stenosis. Any herniation in the NF presses IFL to the SN. Therefore, we think the IFL themselves could cause neurogenic claudication in case of their non-physiological turnover. Visualisation of IFL seems to be possible by using MRI.

## Graphic abstract

These slides can be retrieved under Electronic Supplementary Material.

The graphic abstract consists of three slides from a presentation. The first slide, titled 'Key points', lists three main findings: 1. Intraforaminal ligaments as regular anatomical structures; 2. Stained and plastinated body slices show intraforaminal ligaments; 3. Intraforaminal ligaments are identified in correlating clinical imaging. The second slide, titled 'Ligamental compartments in stained slices and correlating MRI', shows three panels: a PAS-stained slice of a lumbar spine (L4-5) with a red arrow pointing to a horizontal IFL, an MRI T2-sagittal view, and an MRI T2-degad view. The third slide, titled 'Take Home Messages', states that IFLs are revealed by PAS- and Giemsa-stained slices and in correlating clinical imaging, that three compartments (medial, intermedial, lateral) are seen, and that pathological IFL may be diagnosed to find the reason for foraminal stenosis. Each slide includes the journal logo and the authors' names.

**Keywords** Clinical imaging · Intraforaminal ligaments · Radicular pain · Lumbar foraminal stenosis · Plastinated body slices

Dina Wiersbicki and Anna Völker are contributed equally.

**Electronic supplementary material** The online version of this article (<https://doi.org/10.1007/s00586-019-06024-y>) contains supplementary material, which is available to authorized users.

Extended author information available on the last page of the article

## Introduction

Symptoms concerning the lumbar region such as low back pain and radicular pain are often seen in clinical routine having lifetime prevalence up to 50–70% [1]. Lumbar spinal stenosis is found in ~20% of patients with radicular pain

having an increasing prevalence [2]. Therefore, the anatomical region of lumbar neural foramina (NF) has been studied extensively. Spinal nerves (SN), spinal vessels, lymphatics and the recurrent meningeal nerve transmit the NF [3]. Immediately next to these structures, there are ligamentous structures taking course inside the NF. These ligaments are called intraforaminal ligaments (IFL). IFL connect the bordering structures such as lumbar vertebral bodies, intervertebral discs, ligamenta flava, articular processes and the capsule of the facet joint or connect them with the SN. According to the literature, all of these mentioned structures are relevant in lumbar spinal stenosis [4–7].

Of these IFL, contradictory descriptions exist. Caglar's group described them to be inverted-Y-shaped, Akdemir as tunnel-like sheaths of the SN [8, 9]. Consent has been reached only for the existence of the caudal horizontal IFL being visible in magnetic resonance imaging (MRI) [8, 9] and proven by anatomical slices [10]. A connection of the IFL to the lumbar SN, as Akdemir claimed in the literature, contradicts an interpretation of a biomechanical function of these ligaments [9]. How could pathological–anatomical changes be explained, if the regular constitution of the IFL is still being discussed?

In this research, we review the anatomy of the IFL by using newer, highly resolving slice techniques in combination with computed tomography (CT) and MRI.

## Materials and methods

### Preparation and CT/MRI

Fifteen lumbar spines including the first to fifth lumbar vertebrae have been dissected from fresh human bodies (nine females, six males, age 65–94 years; 83.9 years average) by manual preparation to study the IFL of 92 NF. Table 1 shows the analysis of the body donators. While alive, the donor had given consent for the use of body parts for scientific purposes at the Institute of Anatomy, University of Leipzig in accordance with the Saxonian Death and Funeral Act of 1994. No data about lumbar diseases or the environment of the body donators during their lifetime have been available. However, macroscopic pathophysiological changes such as osteophytes near the neural foramina, herniated discs and visible spinal tumours and visible operational interventions at the lumbar spines have been excluded. The donors have been brought to the institute between the first and third day post-mortem.

The bodies have been cooled for the whole time and have been dissected directly after arriving in the Institute of Anatomy. To accelerate the freezing process after dissection, the received specimens have been immersed in 85% acetone at  $-80\text{ }^{\circ}\text{C}$  and afterwards stored in a deep freezer ( $-80\text{ }^{\circ}\text{C}$ ) [11].

**Table 1** Body donators

Gender/age	Lumbar level	Imaging	Plastination group	Cutting plane	Staining	Figures
♀, 65	L1–5	Micro-CT	A	Sagittal	PAS Giemsa	
♂, 92	L1–5 right		A	Horizontal	PAS Giemsa	3 3, 9
♀, 79	L1–5		A	Horizontal	PAS Giemsa	
♂, 69	L2–5		B	Sagittal	PAS Giemsa	
♀, 81	L1–5 left	CT	A	Horizontal	PAS Giemsa	9
♂, 86a	L1–5	CT	B	Horizontal Sagittal	Giemsa	1
♀, 88a	L1–5	CT	B	Sagittal	PAS	2
♀, 85a	L1–5	CT, MRI	B	Sagittal	PAS	6, 8, 9.1, 9.2
♂, 93	L1–5	CT	B	Frontal	PAS	4
♀, 94	L2–5	CT	A	Frontal	PAS	
♀, 88b	L4–5	CT, MRI	B	Frontal	PAS	
♂, 86b	L4–5	CT	A	Oblique	PAS	
♀, 85b	L2–5	CT, MRI	B	Horizontal	PAS	
♀, 90	L2–5	CT, MRI	B	Sagittal	PAS	
♂, 77	L1–5		B	Oblique	PAS	5
♀, 86c	L1–5		Dissection			7

Subsequently, 11 of the spines have been examined with CT (slice thickness 0.67 mm; Brilliance iCT, Philips 100054, Hamburg, Germany). In addition, four of the spines have been analysed with 3-tesla MRI (slice thickness 1.00 mm; MAGNETOM TRIO a Tim System, Siemens, Erlangen, Germany). One T1-weighted sequence (fl2d = FLASH sequence) and two T2-weighted sequences (spc = SPACE sequence and de3d = dual echo sequence) have been performed.

We have defrosted the specimens slowly for the MRI and CT scans [11].

## Dehydration and staining

For the further procedure, the specimens have been divided into groups, A (six specimens): block plastination and B (nine specimens): slice plastination (Table 1).

After dehydration in 100% acetone (Hollborn, Leipzig, Germany) for 3–4 months, block plastinates have been produced from the spines of group A (Table 2; Fig. 1) [11].

Subsequently, the blocks have been sawed into either frontal, horizontal or sagittal slices with a layer thickness down to 800  $\mu\text{m}$  by using a diamond band saw (BS270 S-86, Dramet, Kleinmaischeid, Germany) [11]. Slices of A have been stained alternately with a modified Giemsa method [12] and a staining method with periodic acid–Schiff (PAS) [13].

From the unfixed, frozen specimens of group B, horizontal, frontal, sagittal or oblique slices have been sawed with a thickness  $\sim 1$  mm using a stationary band saw (HL30, Biodur, Heidelberg, Germany, equipped with a 10-mm sawing band from Otto Lange, Leipzig, Germany) [11]. The frozen slices have been stored in 100% acetone (Hollborn, Leipzig, Germany) at  $-80$  °C [11]. The received slices have been stained with the modified Giemsa method mentioned above or with the adjusted PAS reaction (Table 3, Figs. 2, 3, 4, 5) [13].

**Table 2** Figure legend

Sign/colour	Labelled structure
Separate, small arrows	Intraforaminal ligaments (IFL)
Purple →	Connected to spinal nerve
Red →	Not connected, horizontal
Pink →	Not connected, vertical
<span style="border: 1px solid black; padding: 2px;">Brown</span>	Bone
<span style="border: 1px solid black; padding: 2px;">Blue</span>	Ligaments, intervertebral disc
<span style="border: 1px solid black; padding: 2px;">Green</span>	Fascia, dura mater
<span style="border: 1px solid black; padding: 2px;">Orange</span>	Muscle
<span style="border: 1px solid black; padding: 2px;">Red</span>	Vessels, nerves

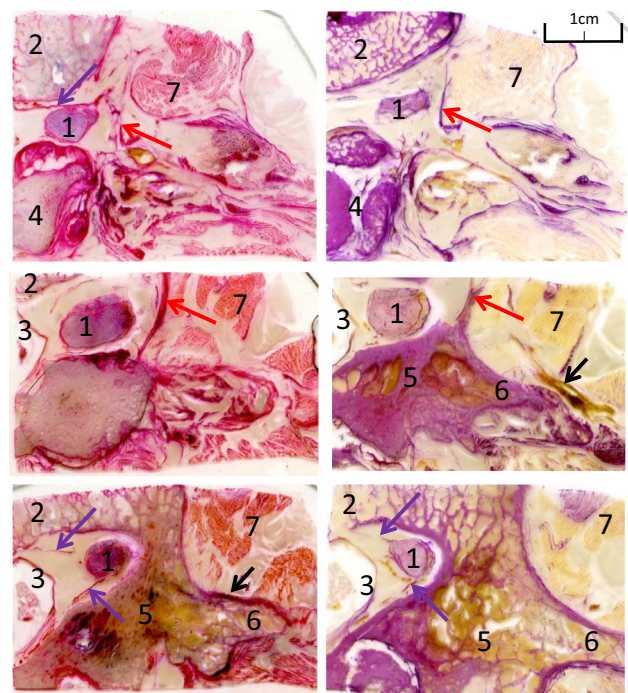


**Fig. 1** Group A: block plastination. Horizontal slices (male, 92 years): first (upper row), third (central row) and fourth (row below) lumbar levels. Left: Giemsa method; right: PAS method. One row contains consecutive slices. Horizontal IFL (red→) and IFL directly touching the nerve (purple→) are cut lengthwise. Spinal nerve (1); vertebral body (2); dura mater (3); facet joints (4); vertebral lamina (5); processus costarius (6); muscle (7); vessels (→)

To sustain the dehydration, the acetone has been renewed biweekly.

## Plastination

The stained slices have been plastinated with epoxy resin (E12/E1, Biodur). Covered with the resin, the slices have been put into a vacuum chamber for 6 h and afterwards embedded between two plastic sheets following the von Hagen's sandwich method (Figs. 1, 2, 3, 4, 5) [11–13]. The plastic sheets have been removed after the resin has hardened to achieve better scans of the embedded slices. For comparison with the corresponding CT and MRI, we have documented the slices with a high-resolution scanner (600–1240 dpi, Scanner EPSON Perfection V750PRO, Epson Deutschland GmbH, 40670 Meerbusch, Deutschland) [11].

## Three-dimensional reconstruction

A three-dimensional model of the lumbar spine has been generated to give an overview of the main types of IFL (Fig. 6). The software Mimics 19.0.0.347 (Materialise GmbH, 82205 Gilching, Deutschland) has been used for

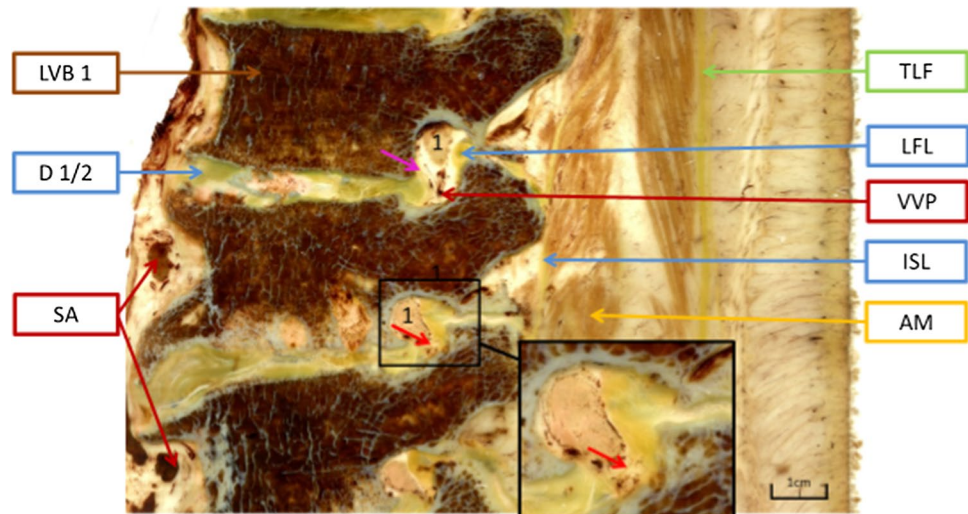
**Table 3** Staining results

	A: block plastination		B: slice plastination	
	PAS <sup>a</sup>	Giemsa	PAS	Giemsa
IFL <sup>b</sup>	Dark violet	Strong pink to red	Pink to slightly red	Light green
Ligamenta flava	Dark violet	Strong pink to red	Pink to red	Green
Ligaments	Dark violet	Strong pink	Pink	Light green
Fascia	Dark violet to purple	Strong pink	Strong pink to red	Light green
Spinal nerve	Bright violet	Violet	Pink to slightly red	Orange–green
Perineurium	Purple	Strong pink	Strong pink	Orange–green
Bone	Purple	Slightly pink	Unstained	Unstained
Periosteum	Dark purple	Violet	Unstained	Light green
Intervertebral disc	Annulus: purple Nucleus: dark purple	(Not in view)	Annulus: strong pink Nucleus: violet	Annulus: green Nucleus: strong green
Muscle	Unstained	Pink to orange	Unstained	Unstained
Vessels	Unstained	Slightly pink	Unstained	Unstained

<sup>a</sup>PAS periodic acid–Schiff (staining)

<sup>b</sup>IFL intraforaminal ligaments

**Fig. 2** Group B: slice plastination. Giemsa-stained sagittal slice (male, 86 years): lumbar spine L1–3: vertical (pink →) and horizontal (red →) IFL lying next to the spinal nerves (1). Lumbar vertebral body (LVB); intervertebral discs (D); vertebral vascular plexus (VVP); thoracolumbar fascia (TLF); autochthonous muscles (AM); interspinous ligaments (ISL); ligamenta flava (LFL); segmental arteries (SA)



this purpose. The data of both block and slice plastinates together with their correlating MRI and CT data have been used.

The bone model has been designed with the MRI and CT data of one specimen (female, 85a, Table 1). The IFL have been transmitted into the bone model by hand as seen in the ~600 plastinated slices of all 15 available specimens of this study (Fig. 6). Each particular lumbar level has been analysed separately using Mimics.

## Dissection

A manual preparation of one thiel-fixed human body (female, age 86) has been conducted [14] showing the

third to fifth lumbar vertebrae with the NF on the right half of the body (Fig. 7).

Thiel's embalming method is based on a diluted salt solution containing ethylene glycol [14]. This technique maintains the colour, texture, plasticity and flexibility similar to a fresh specimen.

## Analysis

The method of planning sample sizes of Rother's group is used to calculate the probability of error by having analysed 15 cases [15].



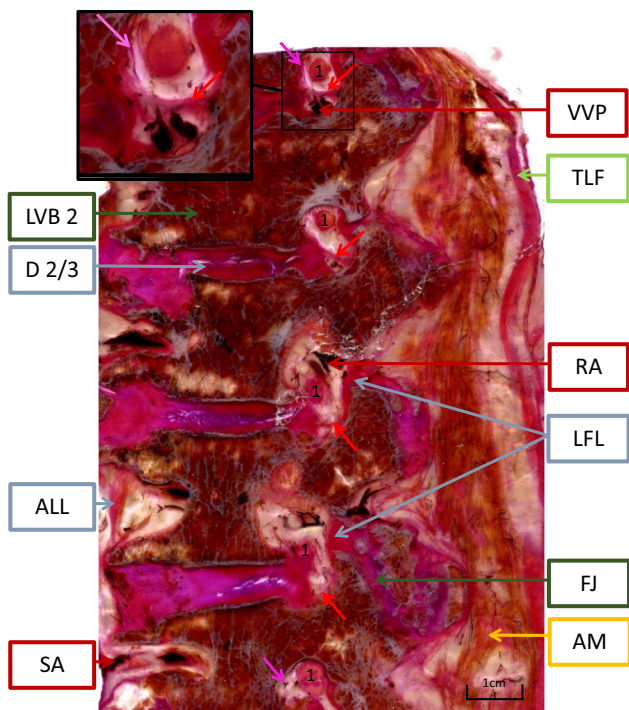


**Fig. 3** Group B: slice plastination. PAS-stained sagittal slice (female, 88 years): lumbar spine L1–5: horizontal (red→) and vertical (pink→) IFL next to spinal nerves (1). Lumbar vertebral bodies (LVB); intervertebral discs (D); ligamenta flava (LFL); facet joints (FJ); vertebral vascular plexus (VVP); radicular artery (RA) of SN 3; anterior longitudinal ligament (ALL); segmental arteries (SA); thoracolumbar fascia (TLF); autochthonous muscles (AM)

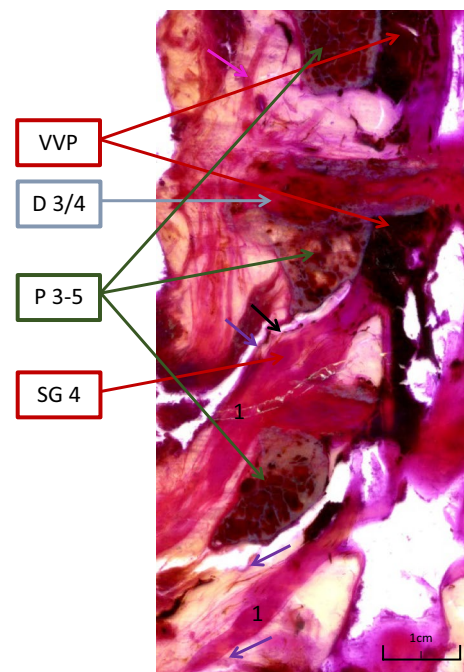


**Fig. 4** Group B: slice plastination. PAS-stained frontal slice (male, 93 years): right lumbar spine L3–5: Spinal ganglion (SG 4) and dura mater (→) in relation to spinal nerves (1) and IFL with direct connection to the nerve (purple→). Pedicles (P); intervertebral discs (D); vertebral vascular plexus (VVP)

## Results

### Preparation

Of the removed lumbar spines, the neural foramina L1/2 to L4/5 have been examined. Three spines have been sliced in the frontal, four in the horizontal, six in the sagittal and two in the oblique section. In total, 92 foramina have been analysed, 16 of L1/2, 24 of both L2/3 and L4/5 and 28 of L4/5 in ~600 slices (Table 1).

### Staining and plastination

The prepared body slices have a thickness of 0.75–2 mm. The integrity of the neuroforaminal structures has been preserved during the process.

The intraforaminal ligaments (IFL) show different directions. Horizontal IFL can be found as one compartment (small red arrows in all figures, cf. Table 2), which have been cut longitudinally in the horizontal (Fig. 1) and sagittal body slices (Figs. 2, 3). They have been found in all horizontal and sagittal cut NF and therefore in 66 NF (ten cases, cf. Table 1).

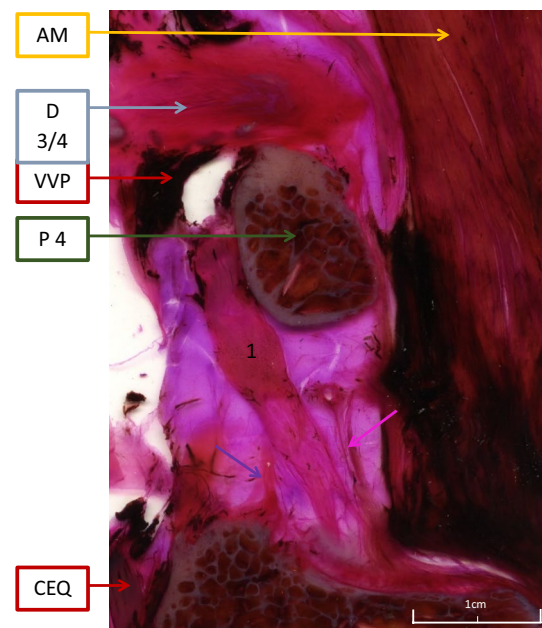


**Fig. 5** Group B: slice plastination. PAS-stained slice (male, 77 years): left lumbar spine L3–5: cut oblique in direction of the spinal nerve (1), vertical IFL (pink→) and IFL with direct contact with the nerve (purple→); intervertebral disc (D); pedicle (P); vertebral vascular plexus (VVP); autochthonous muscle (AM); remains of cauda equina (CEQ) surrounded by cerebrospinal fluid

**Fig. 6** Three-dimensional reconstruction of intraforaminal ligaments (IFL) inside the lumbar neural foramina (NF) L1–L5 using MRI and correlating plastinates. IFL with direct connection to the spinal nerve (1, yellow): dark purple, lying medial; IFL without direct contact with the nerve: pink if vertical (between red and dark purple ligaments), red if horizontal (lateral). 2—Vertebral bodies, 3—intervertebral discs, 4—ligamenta flava. **a** Lateral view from right side, overview of the intraforaminal ligaments, semitransparent, **b** NF L2/3, lateral view, opaque (magnification of **a**, inset), **c** NF L2/3 and L3/4 in frontal view, semitransparent. A supplemental video (online) of the 3D model complements

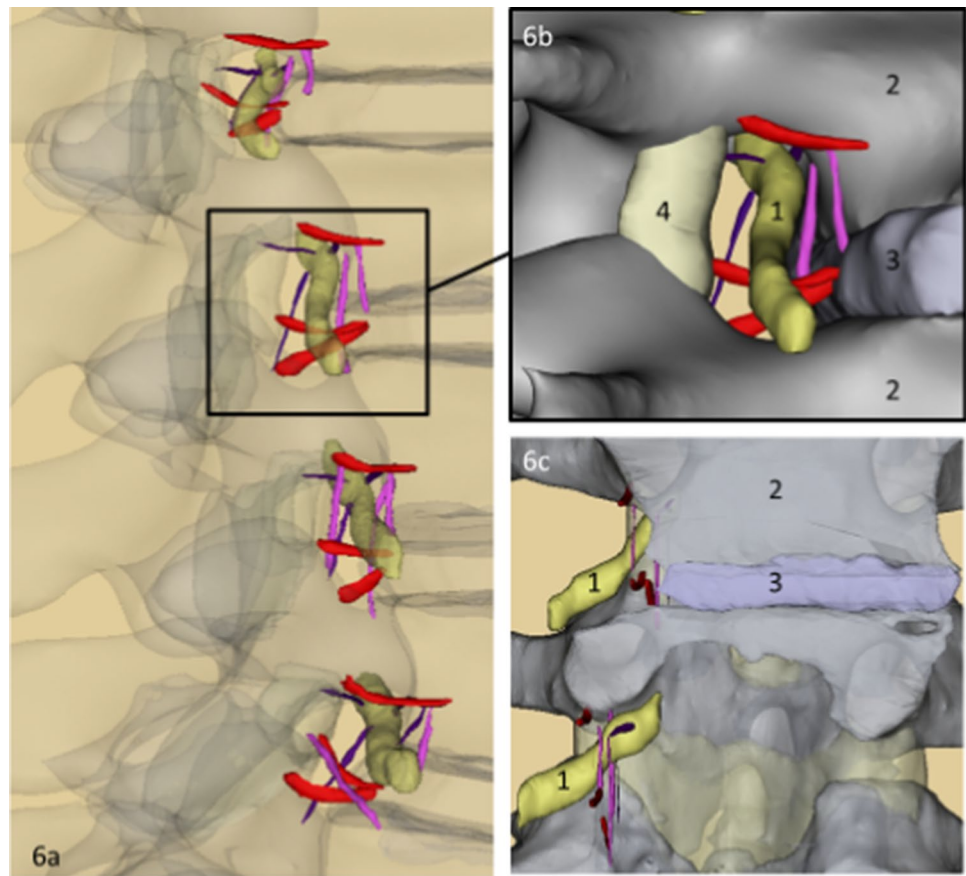
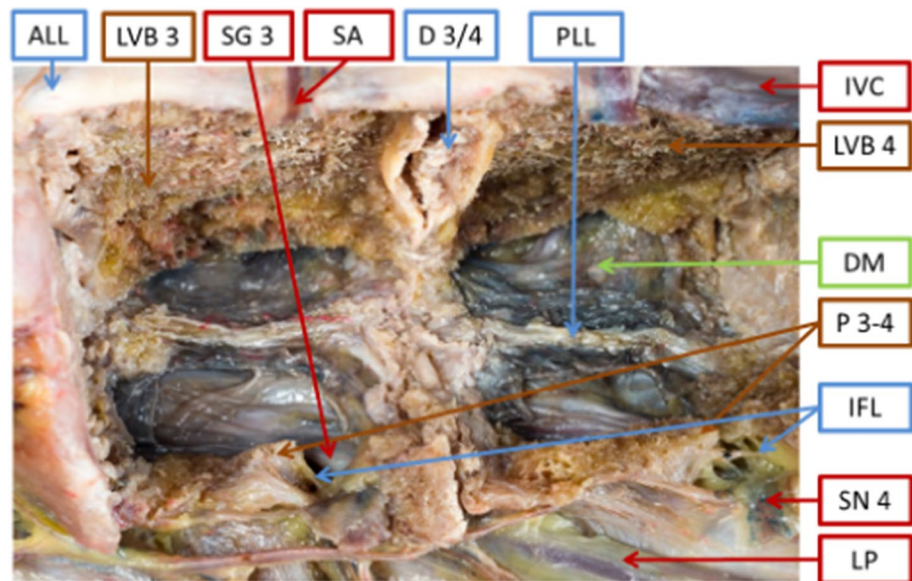


**Fig. 7** Photography. Dissected specimen (female, 86 years): lumbar spine L3–5 viewed from the right. Parts of vertebral bodies (LVB), disc (D), segmental arteries (SA) and anterior longitudinal ligament (ALL) were removed. Spinal nerves (SN) with ligamentous structures (IFL) next to them; pedicles (P); inferior vena cava (IVC); lumbar plexus (LP); posterior longitudinal ligament (PLL); dura mater (DM) partly opened to show spinal ganglion of L3 (SG 3)



Vertical IFL ligaments (small pink arrows in all figures) are visible as another compartment in sagittal (Figs. 2, 3), frontal (Fig. 4) and oblique slices (Fig. 5). They have been found in all sagittal, frontal and oblique NF (68 NF, 11 cases). The horizontal and vertical IFL have no direct

connection to the spinal nerves (SN) (Figs. 1, 2, 3, 4, 5, 6). The horizontal ligaments appear thicker than the vertical ones (Figs. 2, 3).

Additionally, IFL with direct nerve contact with the SN are visualised (small purple arrows in all figures). They can



be seen in horizontal (Fig. 1), frontal (Fig. 4) and oblique slices (Fig. 5) (50 NF, ten cases). The latter are thinner than the IFL without direct nerve connection (Figs. 1, 4, 5). From segments L1/2 to L4/5, all of the IFL increase in thickness (Fig. 1: first to second row). No difference has been detected between left and right side of the body.

**Three-dimensional reconstruction**

The 3D model illustrates the anatomical course of the IFL (Fig. 6, supplemental video). The thin ligaments with direct contact with the SN take course from the dorsal side of the vertebral body and the articular processes to the perineurium of the SN, running from medial to lateral (Fig. 6, purple colour).

The IFL without direct contact with the SN connect the foraminal structures with each other (red and pink arrows in all figures; in 3D model Fig. 6, horizontal: red, vertical: pink). The vertical ligaments connect the pedicles of adjacent vertebrae or the back of the vertebral body with the intervertebral disc. The horizontal IFL are located both cranially and caudally to the SN and link the vertebral body and the articular processes or the capsule of the facet joint and the intervertebral disc. They are located more laterally than the vertical ligaments (Fig. 6).

**MRI/CT**

IFL can be identified in CT and T2-weighted MRI by using the correlating body slices as anatomical reference points (Figs. 8, 9). Again, the diameter of the horizontal IFL is the biggest. They are visible in axial and sagittal MR and axial CT images.

The slightly thinner vertical IFL have been identified in sagittal T2-weighted MRI, but not in CT. The IFL with a

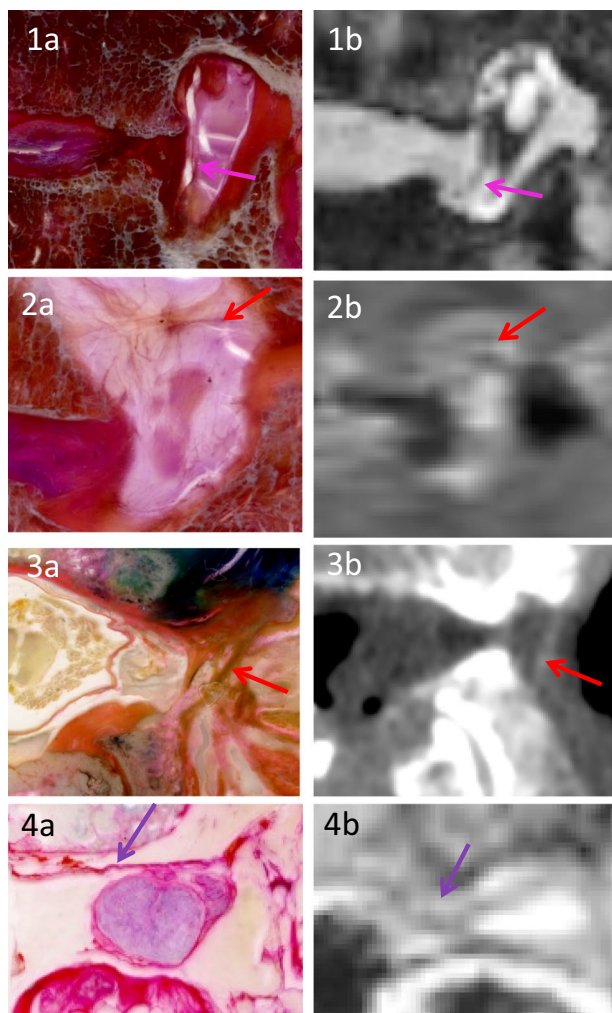


**Fig. 9** Identification of IFL in clinical body imaging with correlating slices: **1a, 2a** sagittal PAS-stained slice; **1b, 2b**: T2-weighted MRI (spc); **3a, 4a**: axial Giemsa-stained slice; **3b**: axial CT; **4b**: axial T2-weighted MRI (spc)

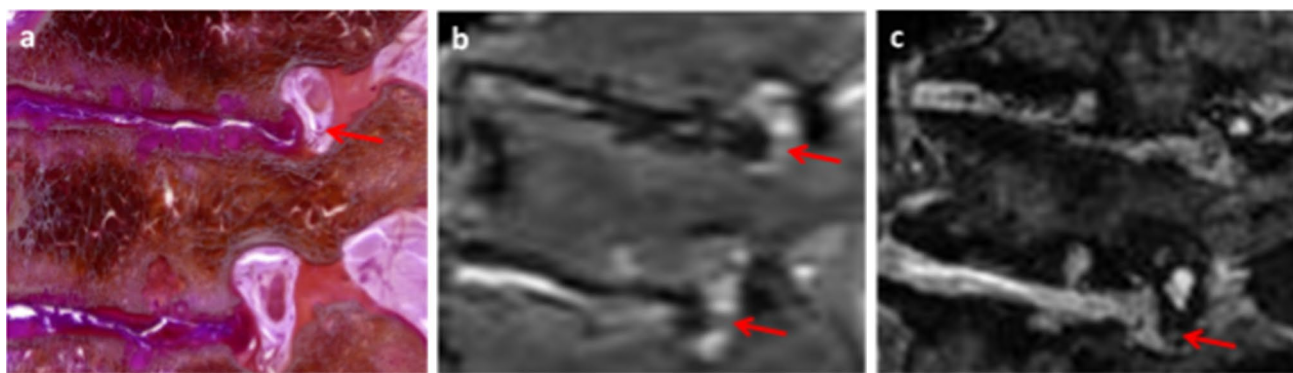


**Fig. 8** Sagittal slices (female, 85 years): lumbar spine L1–3. **a** PAS-stained slice, **b** MRI T2-spc, **c** MRI T2-de3d. →: horizontal IFL

connection to the SN, which are the thinnest of the described ligaments, are seen in axial T2-weighted MRI (Fig. 9).

## Dissection

IFL can be shown using manual dissection. Vertical and horizontal ligaments and ligaments with and without a direct connection to the SN have been displayed in dissection (Fig. 7). All of them except one (\*) have touched the SN.

## Analysis

A probability of error has been calculated about 25% for describing the IFL as anatomical structures using 15 cases [15].

## Discussion

The plastinates show clearly that most of the main intraforaminal ligaments (IFL) have no direct connection to the spinal nerves (SN). This is contradictory to the results of Zhong's group [16]. Their manuscript presented nerve touching ligaments at the entrance zone of the intervertebral foramen. These results were gained by manual dissection having used a medial approach. In our dissection from ventro-lateral, these ligaments seem to also have a connection to the nerve (Fig. 7). However, fewer connections can be seen in the body slices (Table 2; Figs. 1, 2, 3, 4, 5). On plastinates, the thicker ligaments pass the SN.

For example, Zhong's group has shown an IFL lateral to the SN which directly contacts the nerve. In our study, the same ligament at the equal vertebral level is shown in Fig. 1, central row (red arrow); it does not touch the SN. The slices have been sawn from frozen or plastinated blocks [11]; therefore, the resulting offcut may impede seeing the connection between IFL and the SN. Considering that we have examined 15 cases and ~600 slices, it seems implausible for us that we have overseen the main IFL attaching to the SN (cf. Table 1 and supplemental figures). In our view, previous data obtained exclusively by manual dissection (Zhong's group) may overestimate the connections of IFL to the SN. Zhong's group also presents thinner medial ligaments connecting to the nerve. They correspond to our nerve touching ligaments, which are, indeed, thin, and seen medially (Figs. 1, 4, 5, 6, purple arrows/ligaments, supplemental video of 3D reconstruction).

Yuan's group analysed neuroforaminal ligaments also using manual dissection [17]. They referred to ligaments lying more laterally in the intervertebral foramen than the ligaments Zhong's group presented [16]. In similarity to our study, Yuan's group has shown horizontal ligaments taking course cranially and caudally the SN without touching it

(Figs. 1, 2, 3, 6; red). In this sector of the intervertebral foramina thinner vertical ligaments can be found as well (Figs. 2, 3, 4, 5, 6; pink). Yet, they were not seen by Yuan's group.

We think they could not discover these thinner ligaments using manual dissection alone even if they are (unnaturally) indurated due to formaldehyde fixation.

Manual dissection seems to be prone to error due to the mentioned methodical difficulties.

Our dissection shows IFL connected to the SN (Fig. 7). This coincides with the results of others [16, 17]. However, such result does still not reflect the situation in the slices (Figs. 1, 2, 3, 4, 5, 6). The stained plastinates reveal smaller parts of IFL connecting to the SN, while the larger parts do not (Table 2). Due to our data, the main compartments of the IFL pass the lumbar neural foramina freely, not being connected to the SN. All these compartments are visible in standard MRI (Figs. 8, 9).

In our results, we call the intraforaminal ligamentous structures "ligaments" as they are stained in the same colour as common ligaments, (i.e. like the anterior longitudinal ligament and the interspinous ligaments), when using Giemsa and periodic acid–Schiff reaction (PAS) (Table 3; Figs. 2, 3) [12, 13]. Therefore, the IFL, similar to these well-known ligaments, may consist of collagen and transfer loads [18]. Zhong's as are Akdemir's groups indicated that the IFL contain collagen [9, 16]. The PAS-stained ligaments occurred by slice plastination coloured red and pink as the ligamenta flava and the perineurium of the SN are shown in Figs. 3, 4 and 5. Probably IFL protect the SN like the perineurium does, whose structure contains collagen type III [19]. However, neither Akdemir's group, nor Zhong's, nor could we determine the exact types of collagen. This should be done by using specific antibodies via immunohistochemistry in future studies.

According to clinical routine, we have used MRI and CT correlating with the body slices. Direct correlation of each anatomical slice to the imaging has been possible by using the same specimens for radiological analysis and the following plastination process (Fig. 8) [11–13]. Because of MR/CT images and plastinates arising from the same specimen, they can be compared directly [10].

The multiplicity of neuroforaminal structures makes the identification of IFL difficult. In stained slices, the ligaments can be distinguished easily from nerves and vessels (Figs. 1, 2, 3, 4, 5). We have used plastinates to localise the ligaments reliably in the MRI scans (Figs. 8, 9). Nowicki's group alone recognised the importance of slice techniques for identifying IFL in clinical imaging [10]. They studied unstained frozen slices together with body images previously taken from the same specimens to correlate the IFL with clinical imaging. Nowicki's results as ours confirm the hypothesis of Cramer's group that sagittal T2-weighted MRI scans are



most suitable for locating and thus diagnosing IFL (Fig. 8) [20]. Cramer's group identified horizontal IFL caudally to the SN in sagittal MR images and therefore the thickest of the IFL, due to our data (Fig. 8, red arrows). Beyond that Maric's group was able to show horizontal so-called superior corporotransverse ligaments cranially to the SN as well as vertical ligaments in sagittal MR images, as shown in Fig. 9. They again used manual dissection as a correlate [23]. With chosen sagittal body slices, Nowicki's group was able to identify the same horizontal and vertical ligaments as Maric's group in axial and sagittal MR and CT images [10, 21]. In our results, we see the horizontal (red arrows) and vertical (pink arrows) IFL in sagittal T2-weighted MR and axial CT images as well confirming these findings in plastinated slices (Figs. 8, 9). Even the thin IFL with a seen connection to the SN can be visualised in axial MR images (Fig. 9). The used T2 sequences enable a high spatial resolution within an acceptable measurement time. They are used as a standard for orthopaedic spine purposes and are suitable for acquiring high-resolution 3D data sets.

Due to our data, we think that the close topographical relation and the small available space in neural foramina (NF) could cause radicular pain by a thickening of IFL (Figs. 1, 2, 3, 4, 5, 6). As seen here, the IFL and the SN are divided by a small gap, which can be detected in MRI.

Also, the ligaments connected to the SN may change to some extent which is provable using standard MRI (Figs. 8, 9). Any narrowing of the remaining space in the NF brings IFL and SN closer together. Such idea of neural or vascular compression by the IFL is already hypothesised for lumbosacral region [16]. Minimal changes in the IFL could be responsible for this effect.

Huge herniations squeeze the IFL against the SN narrowing the space in-between them and resulting in stenosis with radiological visible hernia. Transformations of the IFL themselves may have the same effect without any visible herniation. The success of therapeutic procedures confirms this hypothesis. Pereira's group experienced pain relief after secondary dilation of the NF for patients with persistent pain after decompression [22]. Overall, the IFL seem to be involved in all types of stenosis [4, 6]. Therefore, a so-called occult stenosis would not exist, if in the clinical diagnosis the IFL could be ascertained as pain generator.

## Limitations

Considering the comparatively low number of specimen, a probability of error has been calculated to 25% using 15 cases for describing the IFL compartments [15]. A secondary proof of our description arises by the MRI data of specimens which appear to be macroscopically normal, where all three compartments of IFL are visible (Figs. 8, 9).

The applied method is limited by the advanced age of the body donators (83.9 years average), which implicates physiological degeneration of ageing. According to German ethical standards and Saxonian Death and Funeral Act of 1994, the patient has to be at least 65 years old when dying for becoming a body donator. However, relevant degeneration or diseases were not diagnosed by the experienced physicians contributing to this study (C.E.H.; A.V.). Macroscopic pathophysiological changes and operational interventions at the lumbar spines were excluded.

**Acknowledgements** Our sincere thanks are due to the association "Deutsche Arthrose-Hilfe e.V.", which has funded this study, and Mrs. Charlotte Kulow (Institute for Anatomy, University Leipzig) for proof-reading. Mrs. Heike Röder (Institute for Radiology, University Leipzig) has helped with CT/MRI scans and Ms. Marie Lynn Speckert and Mr. Thomas Wolfskämpf in staining and plastination process. Ms. Anna Katharina Rowedder made the photograph of the dissected specimen.

## Compliance with ethical standards

**Conflict of interest** The authors declare that they have no conflicts of interests.

## References

1. Duthey B (ed) (2004) Priority medicines for Europe and the world 'A public health approach to innovation', vol 2013. WHO, Geneva
2. Kalichman L, Cole R, Kim DH, Li L, Suri P, Guermazi A, Hunter DJ (2009) Spinal stenosis prevalence and association with symptoms: the Framingham Study. *Spine J* 9(7):545–550. <https://doi.org/10.1016/j.spinee.2009.03.005>
3. Gilchrist RV, Slipman CW, Bhagia SM (2002) Anatomical review. *Pain Physician* 5(4):372–378
4. Splendiani A, Ferrari F, Barile A, Masciocchi C, Gallucci M (2014) Occult neural foraminal stenosis caused by association between disc degeneration and facet joint osteoarthritis: demonstration with dedicated upright MRI system. *Radiol Med* 119(3):164–174. <https://doi.org/10.1007/s11547-013-0330-7>
5. Ishimoto Y, Yoshimura N, Muraki S, Yamada H, Nagata K, Hashizume H, Takiguchi N, Minamide A, Oka H, Kawaguchi H, Nakamura K, Akune T, Yoshida M (2013) Associations between radiographic lumbar spinal stenosis and clinical symptoms in the general population: the Wakayama Spine Study. *Osteoarthritis Cartil* 21(1063–4584):783–788. <https://doi.org/10.1016/j.joca.2013.02.656>
6. Nowicki BH, Houghton VM, Schmidt TA, Lim T-H, An HS, Riley LH III, Yu L, Hong J-W (1996) Occult lumbar lateral spinal stenosis in neural foramina subjected to physiologic loading. *AJNR Am J Neuroradiol* 17(0195–6108/96):1605–1614
7. Qian Y, Qin A, Zheng MH (2011) Transforaminal ligament may play a role in lumbar nerve root compression of foraminal stenosis. *Med Hypotheses* 77:1148–1149
8. Caglar YS, Dolgun H, Caglar Ugur H, Kahilogullari G, Tekdemir I, Elhan A (2004) A ligament in the lumbar foramina: inverted Y ligament—an anatomic report. *Spine* 29(14):1504–1507
9. Akdemir G (2010) Thoracic and lumbar intraforaminal ligaments: laboratory investigation. *J Neurosurg Spine* 13(3):351–355

10. Nowicki BH, Haughton VM (1992) Neural foraminal ligaments of the lumbar spine: appearance at CT and MR imaging. *Radiology* 183(1):257–264
11. Kürtül I, Hammer N, Rabi S, Saito T, Bohme J, Steinke H (2012) Oblique sectional planes of block plastinates eased by Sac plastination. *Ann Anat* 194(0940–9602):404–406. <https://doi.org/10.1016/j.aanat.2011.11.006>
12. Steinke H, Rabi S, Saito T (2008) Staining body slices before and after plastination. *Eur J Anat* 12(1):51–55
13. Steinke H, Wiersbicki D, Speckert M-L, Merkwitz C, Wolfskämpf T, Wolf B (2017) Periodic acid-Schiff (PAS) reaction and plastination in whole body slices. A novel technique to identify fascial tissue structures. *Ann Anat* 216:29–35. <https://doi.org/10.1016/j.aanat.2017.10.001>
14. Thiel W (1992) Die Konservierung ganzer Leichen in natürlichen Farben [The preservation of the whole corpse with natural color]. *Ann Anat* 174(3):185–195 (in German)
15. Rother P, Jahn W (1989) Stichprobenplanung in der Morphometrie [Random sample planning in morphometry]. *Gegenb Morph Jb* 135(1):121–124 (in German)
16. Zhong E, Zhao Q, Shi B, Xie Y, Ding Z, Lv H, Zhong S, Huang W (2018) The morphology and possible clinical significance of the intraforaminal ligaments in the entrance zones of the L1–L5 levels. *Anatomic study. Pain Physician* 21:E157–E165
17. Yuan S-G, Wen Y-L, Zhang P, Li Y-K (2015) Ligament, nerve, and blood vessel anatomy of the lateral zone of the lumbar intervertebral foramina. *Int Orthop* 39(11):2135–2141. <https://doi.org/10.1007/s00264-015-2831-6>
18. Pauwels F (1980) Biomechanics of the locomotor apparatus: contributions on the functional anatomy of the locomotor apparatus. Springer, Berlin
19. D'Ardenne AJ, McGee JO (1984) Fibronectin in disease. *J Pathol* 142(4):235–251. <https://doi.org/10.1002/path.1711420402>
20. Cramer GD, Skogsbergh DR, Bakkum BW, Winterstein JF, Yu S, Tuck NR (2002) Evaluation of transforaminal ligaments by magnetic resonance imaging. *J Manip Physiol Ther* 25(4):199–208. <https://doi.org/10.1067/mmt.2002.123174>
21. Maric DL, Krstonosic B, Eric M, Maric DM, Stankovic M, Milosevic NT (2015) An anatomical study of the lumbar external foraminal ligaments: appearance at MR imaging. *Surg Radiol Anat* 37(1):87–91
22. Pereira P, Severo M, Monteiro P, Silva PA, Rebelo V, Castro-Lopes JM, Vaz R (2016) Results of lumbar endoscopic adhesiolysis using a radiofrequency catheter in patients with postoperative fibrosis and persistent or recurrent symptoms after discectomy. *Pain Pract* 16(1):67–79. <https://doi.org/10.1111/papr.12266>

**Publisher's Note** Springer Nature remains neutral with regard to jurisdictional claims in published maps and institutional affiliations.

## Affiliations

Dina Wiersbicki<sup>1</sup> · Anna Völker<sup>2</sup> · Christoph-Eckhard Heyde<sup>2</sup> · Hanno Steinke<sup>1</sup> 

✉ Hanno Steinke  
steinke@medizin.uni-leipzig.de

Dina Wiersbicki  
Dina.Wiersbicki@medizin.uni-leipzig.de

Anna Völker  
Anna.Voelker@medizin.uni-leipzig.de

Christoph-Eckhard Heyde  
Christoph-Eckhard.Heyde@medizin.uni-leipzig.de

<sup>1</sup> Institute for Anatomy, Leipzig University, Liebigstr. 13, 04103 Leipzig, Germany

<sup>2</sup> Clinic for Orthopaedics, Trauma Surgery and Plastic Surgery, Department of Spine Surgery, University Hospital Leipzig, Liebigstr. 20, 04103 Leipzig, Germany